AGU PUBLICATIONS

Geophysical Research Letters

RESEARCH LETTER
10.1002/2014GL062107

Key Points:
- A reduction in sea ice near a major Greenland fiord began in the mid-1990s
- This reduction was associated with the regional warming of the subpolar gyre
- The Icelandic and Lofoten Lows are associated with regional climate variability

Supporting Information:
- Text S1
- Figures S1–S4

Correspondence to:
G. W. K. Moore,
gwk.moore@utoronto.ca

Citation:
Moore, G. W. K., F. Straneo, and M. Oltmanns (2014), Trend and interannual variability in southeast Greenland Sea Ice: Impacts on coastal Greenland climate variability, *Geophys. Res. Lett.*, *41*, 8619–8626, doi:10.1002/2014GL062107.

Received 4 OCT 2014
Accepted 4 NOV 2014
Accepted article online 7 NOV 2014
Published online 2 DEC 2014

Trend and interannual variability in southeast Greenland Sea Ice: Impacts on coastal Greenland climate variability

G. W. K. Moore[1], F. Straneo[2], and M. Oltmanns[2]

[1]Department of Physics, University of Toronto, Toronto, Ontario, Canada, [2]Department of Physical Oceanography, Woods Hole Oceanographic Institution, Woods Hole, Massachusetts, USA

Abstract We describe the recent occurrence of a region of diminished sea ice cover or "notch" offshore of the Kangerdlugssuaq Fiord, the site of the largest tidewater glacier along Greenland's southeast coast. The notch's location is consistent with a topographically forced flux of warm water toward the fiord, and the decrease of the sea ice cover is shown to be associated with a regional warming of the upper ocean that began in the mid-1990s. Sea ice in the vicinity of the notch also exhibits interannual variability that is shown to be associated with a seesaw in surface temperature and sea ice between southeast and northeast Greenland that is not describable solely in terms of the North Atlantic Oscillation. We therefore argue that other modes of atmospheric variability, including the Lofoten Low, are required to fully document the changes to the climate that are occurring along Greenland's east coast.

1. Introduction

The marginal ice zone (MIZ), the transitional region that separates the dense pack ice from the open water, is a region where a number of climatologically important processes, such as air-sea ice interaction, occur [*Renfrew and Moore*, 1999; *Strong*, 2012] and where significant biological activity takes place [*Grebmeier et al.*, 1995]. The MIZ is typically defined as the region where sea ice concentration is between 15% and 80%, and the subpolar North Atlantic has such zones in the Labrador, Irminger, Iceland, Greenland, and Barents Seas [*Strong*, 2012]. In addition to the loss of multiyear sea ice from the Arctic Ocean [*Parkinson and Cavalieri*, 2008], there has also been a loss of winter sea ice in the marginal seas of the North Atlantic that has been manifested as a reduction in the width of the MIZs [*Strong*, 2012; *Strong and Rigor*, 2013].

There is also evidence of significant interannual variability in the characteristics of the MIZs of the subpolar North Atlantic [*Chapman and Walsh*, 1991; *Strong*, 2012]. The North Atlantic Oscillation (NAO) plays a role in forcing this variability, but it does not fully describe it [*Strong*, 2012]. *Deser et al.* [2000] identified an out-of-phase relationship or seesaw in winter sea ice extent between the Greenland and Labrador Seas. Although the NAO plays an important role in forcing this seesaw, the relationship with the NAO identified by *Deser et al.* [2000] does not hold for all winters, again suggesting that other regional atmospheric circulation patterns play a role in this mode of interannual variability [*Hurrell and Deser*, 2009].

Sea ice is exported out of the Arctic via Fram Strait [*Kwok et al.*, 2004] and advected southward by the east Greenland Current along the east coast of Greenland, with a progressive decrease in sea ice concentration [*Chapman and Walsh*, 1991]. The presence of sea ice exerts a strong influence on the regional climate, and southeast Greenland is colder compared to the same latitude in west Greenland as a result. Variations in sea ice along the coast impact local populations by affecting hunting, fishing, and the arrival of the cargo ships that replenish their supplies [*Instanes*, 2005]. It also affects marine ecosystems by limiting light availability [*Grebmeier et al.*, 1995; *Nuttall*, 2005]. In addition, the presence of sea ice along the coast and in the glacial fjords of Greenland may exert a stabilizing impact on the large tidewater glaciers located in this region by combining with icebergs to form an ice mélange that inhibits calving [*Howat et al.*, 2011; *Walter et al.*, 2012] or by influencing the regional climate [*Murray et al.*, 2010].

Therefore, a reduction of sea ice from Greenland's coastal region may have contributed to a reduction in the cold fresh waters transported over the upper 100–150 m by the east Greenland Current and facilitated by the intrusion of subsurface warm Atlantic waters onto the shelf and into the glacial fjords. Enhanced warm water intrusion may have led to increased submarine melting at the edge of the glaciers

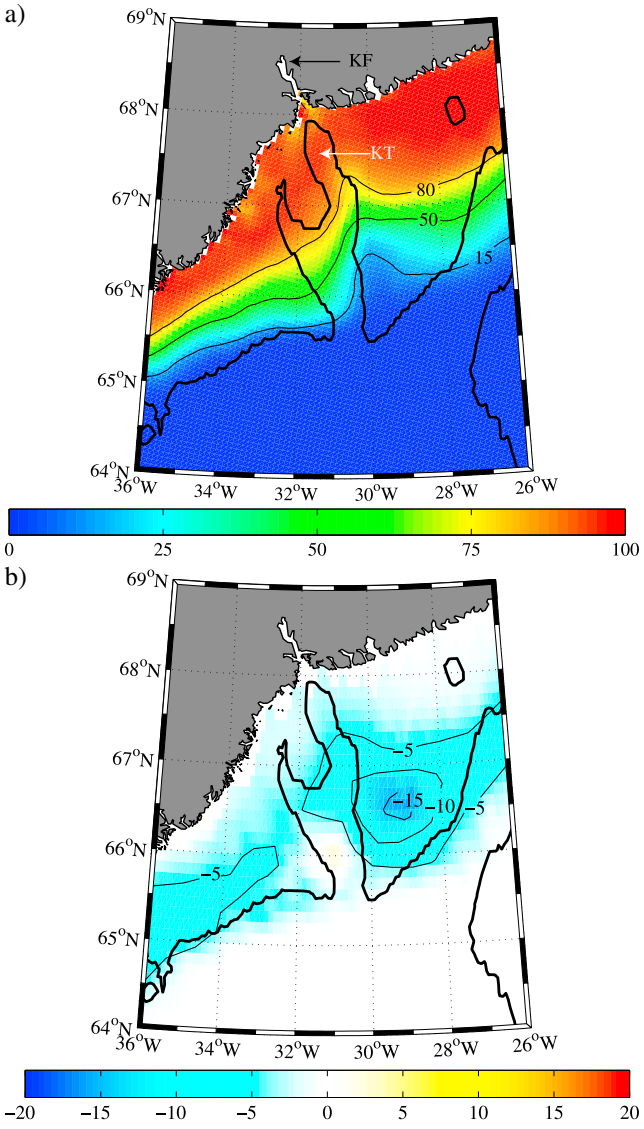

Figure 1. Sea ice conditions in the vicinity of the Kangerdlugssuaq Fiord southeast Greenland. (a) The winter mean (JFM) sea ice concentration (%) from the AMSR-E data set during the period 2003–2011. (b) The difference in winter mean sea ice concentration (%) from the Bootstrap data set between the periods 2003–2012 and 1979–1988. The thick black contour is the 400 m isobath. The location of the Kangerdlugssuaq Fiord (KF) and the Kangerdlugssuaq Trough (KT) are indicated in Figure 1a.

[*Straneo et al.*, 2010; *Christoffersen et al.*, 2011]. Thus, this reduction in sea ice may have been a factor in the recent accelerated retreat of these glaciers that represents a significant contribution to the observed mass loss from the Greenland Ice Sheet [*Straneo and Heimbach*, 2013; *Straneo et al.*, 2013]. Support for a link between sea ice extent along the Greenland coast and the retreat of one major tidewater glacier is provided by the analysis of sediment core data collected near the glacier terminus [*Andresen et al.*, 2012].

In this paper, we describe a localized region of reduced sea ice cover or "notch" that developed during the mid-1990s within the MIZ on the eastern flank of the Kangerdlugssuaq Trough (KT) offshore of the Kangerdlugssuaq Fiord (KF), the site of one of the large tidewater glaciers that have recently accelerated and retreated [*Howat et al.*, 2011]. We will argue that the development of this notch is the result of the topographically controlled inflow of warm subtropical water along the submarine trough that connects the fiord to the deep ocean. We will also show that there is interannual variability on the 2–8 year time scale in sea ice cover in the vicinity of the notch that is associated with the Lofoten Low, a regional atmospheric circulation feature that is distinct from the Icelandic Low [*Jahnke-Bornemann and Bruemmer*, 2009; *Moore et al.*, 2012]. Finally, we identify a hitherto unidentified seesaw in sea ice concentration along the southeast and northeast coasts of Greenland that is associated with a large-scale thermal oscillation between the Greenland Ice Sheet and northern Scandinavia that is again associated with variability in the Lofoten Low.

2. Results

Figure 1a shows the winter mean (January-February-March (JFM)) sea ice concentration in the vicinity of the KF as represented in the Advanced Microwave Scanning Radiometer–EOS (AMSR-E) data set for the period 2003–2011 [*Spreen et al.*, 2008]. The notch can be seen as the localized region of reduced sea ice concentration that extends across the MIZ and into the pack ice offshore of the fiord. The bathymetry in the region is also shown, and it can be seen that the notch is situated along the eastern side of the KT that cuts across the continental shelf and connects the KF to the deep ocean. This feature is also present in the longer-term Bootstrap [*Comiso and Sullivan*, 1986] as well as the NASA Team [*Cavalieri et al.*, 2013]

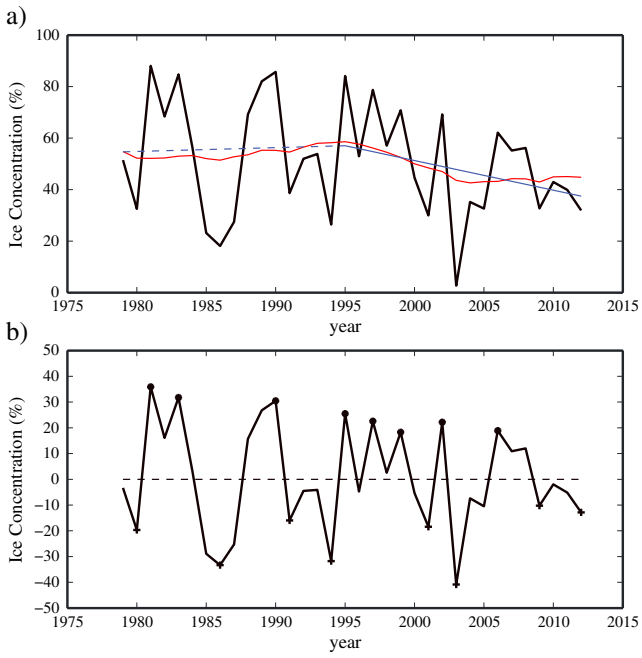

Figure 2. Variability in sea ice conditions near the Kangerdlugssuaq notch 1979–2012. (a) The time series of winter mean (JFM) sea ice concentration in the vicinity of the notch. The red curve represents the SSA low-frequency reconstruction of this time series. The dashed and solid blue lines represent the piecewise linear least squares fit to the time series with a breakpoint in 1995. The trend during the period prior to the breakpoint was not statistically significant. (b) The SSA interannual reconstruction of this time series. The extrema for this reconstruction are indicated by the "dot" and "cross" markers.

sea ice concentration data sets. The difference in winter mean sea ice concentration, as represented in the Bootstrap data set, between the periods 2003–2012 and 1979–1988 is shown in Figure 1b. It confirms that the largest reduction in regional sea ice concentration occurred on the eastern side of the KT offshore of and extending toward the fiord's mouth. Similar results were obtained with the NASA Team data set.

A time series of the winter mean sea ice concentration in the vicinity of the Kangerdlugssuaq sea ice notch, defined as the area average of the sea ice concentration in the region where the magnitude of the difference field shown in Figure 1b exceeded 10%, is shown in Figure 2a. Details on the temporal evolution of this time series were identified using the singular spectrum analysis (SSA) technique that decomposes a time series into components without any a priori assumptions about their parametric form [*Ghil et al.*, 2002].

The SSA decomposition of this time series indicates the presence of a low-frequency mode that explains ~10% of the variance as well as two modes, appearing in quadrature—a characteristic that is usually indicative of oscillatory phenomenon [*Ghil et al.*, 2002], with periods of ~8 and ~2.5 years that, respectively, explain ~52% and ~27% of the variance. The SSA reconstruction of the low-frequency mode of variability is also shown in Figure 2a. It indicates that during the period from 1979 to the mid-1990s, there was no trend in the time series and that after that date, there was a decreasing trend. This behavior was confirmed with a piecewise continuous linear least squares fit to the time series with a prescribed breakpoint in 1995, selected on the basis of the SSA results, that is also shown in Figure 2a. The statistical significance of the piecewise trends was assessed with a Monte Carlo technique that used 10,000 synthetic time series with the same spectral characteristics as the underlying time series [*Rudnick and Davis*, 2003; *Moore*, 2012]. This test indicated that the trend in the period prior to 1995 was not statistically significant while that after 1995 was statistically significant at the 99% confidence interval. Other breakpoints consistent with the behavior of the SSA decomposition yielded similar results.

Figure 2b shows the interannual variability in the winter mean sea ice concentration in the vicinity of the sea ice notch that was obtained by subtracting out the low-frequency SSA reconstruction from the full time series. This detrended time series shows evidence of interannual variability with evidence of a shift toward higher-frequency variability that occurred in the mid-1990s. This behavior was confirmed by an inspection of the SSA reconstruction of the 8 year mode that showed a reduction in its amplitude in the mid-1990s (Figure S1 in the supporting information).

Figure 3 shows the spatial correlation coefficient of the winter mean sea surface temperature (SST) from the advanced very high resolution radiometer optimal interpolation data set [*Reynolds et al.*, 2007] against both the SSA low-frequency and interannual reconstructions of the winter mean sea ice concentration in the vicinity of the sea ice notch. Care must be taken in interpreting the correlations where sea ice is present as the

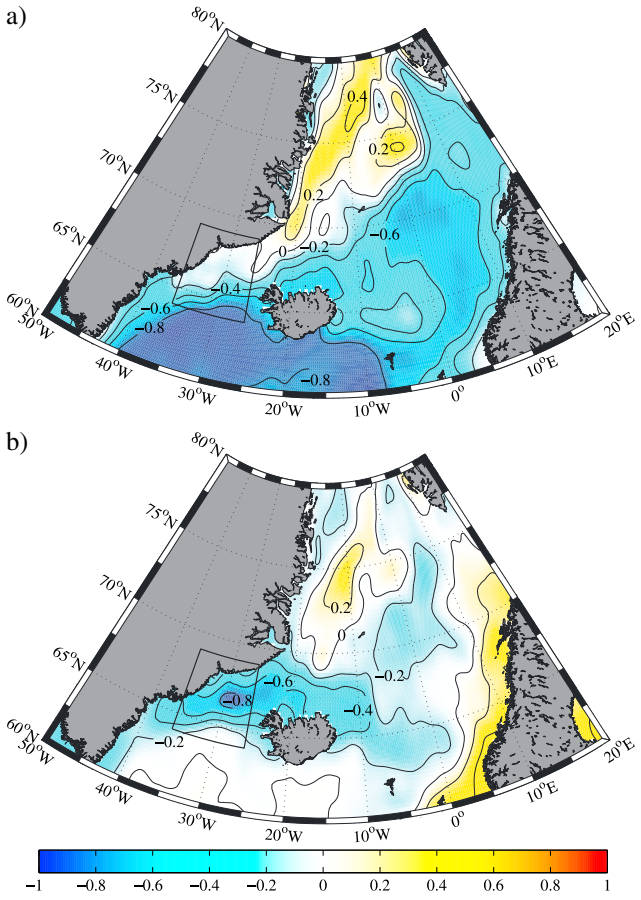

Figure 3. Spatial correlation coefficient of the winter mean (JFM) Reynolds sea surface temperature field with (a) the low-frequency and (b) the interannual SSA reconstruction of winter mean (JFM) sea ice concentration in the vicinity of the Kangerdlugssuaq notch for the period 1982–2012. The domain shown in Figure 1 is indicated.

SST in these regions is a blend of observations and a prescribed functional dependence of sea ice concentration [*Reynolds et al.*, 2007]. The correlation with the low-frequency reconstruction (Figure 3a) is large and negative over the subpolar gyre, indicating that the decrease in sea ice concentration that has occurred since the mid-1990s is associated with a surface warming in this region over the same period of time. This result is consistent with the observed warming of the upper half kilometer of the subpolar gyre [*Straneo and Heimbach*, 2013]. In contrast, along the northeast coast of Greenland, the correlation is positive, indicating that the loss of sea ice in the vicinity of the notch is associated with a surface cooling in this region. The correlation with the interannual reconstruction (Figure 3b) indicates a more localized region in the vicinity of the sea ice notch where there is a large anticorrelation. There is also a region of positive correlation along the northeast coast of Greenland. The correlation coefficient in the winter mean SST between these two regions is O(−0.5), confirming the existence of a seesaw in SST between the southeast and northeast coasts of Greenland that is associated with the interannual variability in sea ice that we have identified.

Turning now to the atmospheric circulation anomalies associated with the interannual variability in the sea ice notch, we show in Figure 4 the composite winter mean sea level pressure, 10 m wind, and 2 m air temperature fields, all from the ERA-1 [*Dee et al.*, 2011], for the identified maxima and minima in this mode of variability that are indicated in Figure 2b. The high sea ice composite (Figure 4a) has two minima in the sea level pressure field, with one near 62°N, 30°W that is associated with the Icelandic Low and the other near 70°N, 5°W that is associated with the Lofoten Low. For this composite, the Icelandic Low is ~1 mbar lower than its climatological value, while the sea level pressure in the vicinity of the Lofoten Low is ~4 mbar lower than climatology (Please refer to the climatological fields shown in Figure S2 in the supporting information). As a result, there is an enhanced barrier flow along the northeast and southeast coasts of Greenland that, due to the frictional turning of the surface wind [*Holton*, 2004], results in an enhanced off-ice edge flow. In contrast, the low sea ice composite (Figure 4b) is characterized by single-pressure minimum, the Icelandic Low centered near 60°N, 40°W, and a trailing trough that extends northeastward toward the Barents Sea. As a consequence, the surface flow along the east coast of Greenland is weaker and does not have a pronounced offshore component.

The difference in the two composites is shown in Figure 4c and indicates that interannual variability in sea ice in the vicinity of the sea ice notch is associated with circulation anomalies that extend across the Nordic Seas. In particular, there is a large (~8 mbar) difference in sea level pressure in the vicinity of the Lofoten Low between the high and low states. The cyclonic circulation anomaly results in enhanced northerly flow along the entire east Greenland MIZ. This circulation anomaly is also associated with enhanced flow along the eastern margin of the Greenland Ice Sheet that is focused into enhanced outflow

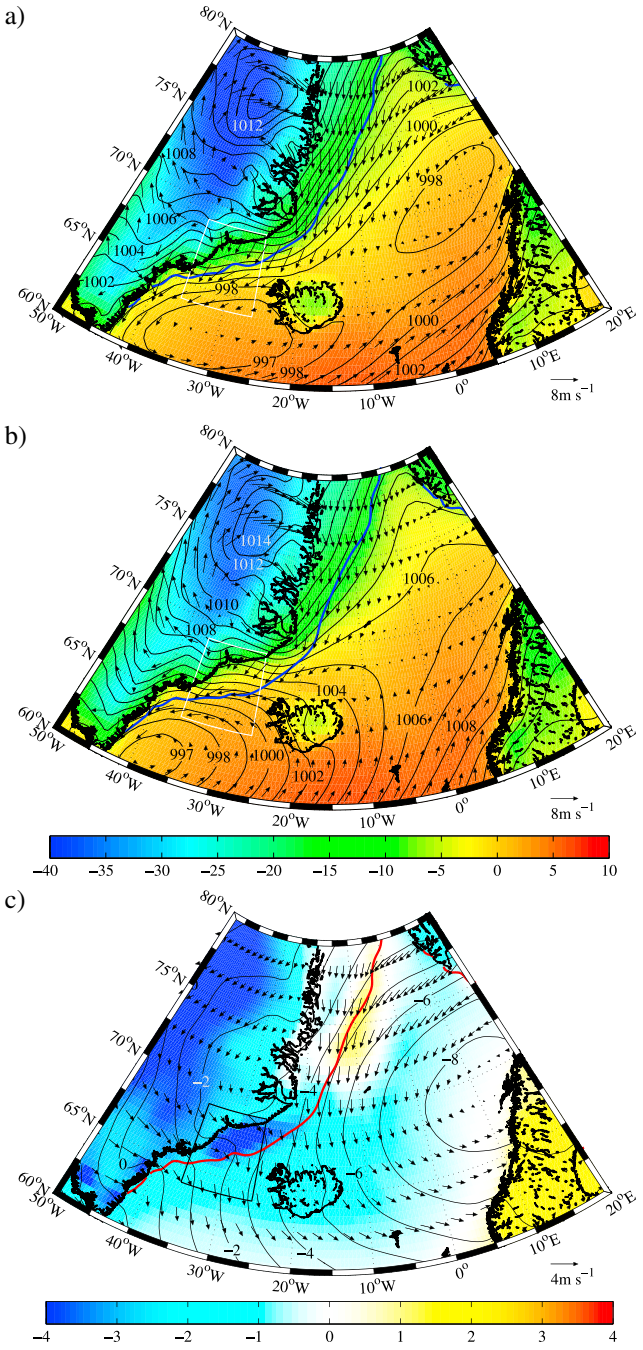

Figure 4. Composite sea level pressure (contours: mbar), 10 m wind (vectors: m/s), and 2 m air temperature (shading: °C) during (a) high and (b) low periods in the SSA interannual reconstruction of winter mean sea ice concentration in the vicinity of the Kangerdlugssuaq notch. (c) The difference in the high and low composites. The thick blue curves in Figures 4a and 4b represent the respective composite 50% sea ice concentration contours. In Figure 4c, the thick red curve represents the winter mean 50% sea ice contour. All fields are winter means (JFM) from the ERA-1. The domain shown in Figure 1 is indicated.

along the large fiords of southeast Greenland [*Oltmanns et al.*, 2014]. There is also a pronounced temperature anomaly across the entire region with surface air temperatures over Greenland being ~4°C colder and those over Scandinavia being ~4°C warmer in the high state as compared to the low state. The Greenland thermal anomaly extends over the sea ice notch indicating that, as expected, surface air

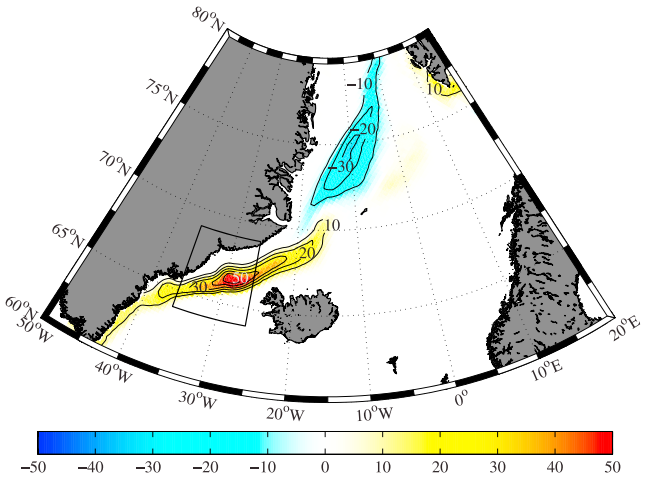

Figure 5. Difference in the winter mean composite sea ice concentration (%) during the high and low periods in the SSA interannual reconstruction of winter mean sea ice concentration in the vicinity of the Kangerdlugssuaq notch. The domain shown in Figure 1 is indicated.

temperatures are colder during the high phase as compared to the low phase. There is also a thermal anomaly of opposite sign along the northeast Greenland MIZ.

Finally, we show in Figure 5 the difference in the composite winter sea ice concentration between the high and low states of the interannual oscillation in sea ice concentration in the vicinity of the sea ice notch. From the figure, one can see evidence of a seesaw in sea ice concentration between the southeast and northeast coasts of Greenland. This seesaw is restricted to the MIZ and hence is closer to shore along the southeast coast of Greenland and is farther offshore along the northeast coast.

3. Discussion

In this paper, we have described the variability that is associated with a local minimum in sea ice that occurs offshore of the KF. The sea ice concentration in its vicinity has been shown to exhibit a large degree of interannual variability on time scales from 2 to 8 years that is superimposed on a trend toward lower sea ice concentrations that began in the mid-1990s. This trend is responsible for the formation of the pronounced notch in sea ice in the region. This low-frequency behavior was identified with the SSA and confirmed with a continuous piecewise linear least squares fit.

This low-frequency behavior was shown to be associated with a large-scale warming of surface and subsurface waters of the subpolar North Atlantic that began in the mid-1990s and was the result of an anomalously large inflow of warm subtropical water into the region [*Hakkinen and Rhines*, 2004]. It has been proposed that this augmented influx of warm water contributed to the acceleration and the retreat of large tidewater glaciers, grounded several hundreds of meters below sea level, along the southeast coast of Greenland that began around 2000 [*Holland et al.*, 2008; *Straneo et al.*, 2010; *Christoffersen et al.*, 2011; *Howat et al.*, 2011]. Generally, this warm water is trapped offshore along the continental shelf within the Irminger Current, while the colder water of polar origin is typically situated closer to shore [*Straneo et al.*, 2010]. The presence of deep troughs, such as KT, allows these warm waters to penetrate onto the shelf [*Sutherland et al.*, 2014]. A reduction in the amount of cold freshwater of polar origin is associated with an increase in the warm waters that penetrate in the fjords on seasonal, interannual, and decadal time scales [*Straneo et al.*, 2010; *Andresen et al.*, 2012]. The low-frequency behavior of the sea ice conditions in the vicinity of the sea ice notch is consistent with this view. While we have no direct evidence, the reduction in sea ice is likely associated with the increased influx of increased warm Atlantic water onto the shelves.

Similar features exist in the vicinity of other large fiords along the southeast coast of Greenland. These notches are typically situated along the eastern edges of the associated submarine troughs (Figure S3 in the supporting information), consistent with the topographic control that constrains the warm inflow to the eastern side of the troughs [*Sutherland and Pickart*, 2008; *Sutherland and Cenedese*, 2009]. Thus, the processes described in this paper may also be occurring at these fiords as well.

We have also identified large-amplitude interannual variability in wintertime sea ice in the vicinity of the Kangerdlugssuaq sea ice notch. This variability is associated with a seesaw in sea ice concentration between the southeast and northeast coasts of Greenland that is consistent with the patterns seen in the SST and surface air temperature fields. It also suggests that it may play a role in modulating the regional climate of this region potentially affecting the ice sheet's outlet glaciers. This interannual variability is associated with large-scale circulation anomalies over the subpolar North Atlantic. However, the leading order anomalies are

not associated with the Icelandic Low but rather with the Lofoten Low. This suggests that the hypothesis put forth by *Christoffersen et al*. [2011] that variability in the location of the Icelandic Low controls the warm water intrusion into the KF requires a revision to take into account the role played by the Lofoten Low.

The variability associated with the Lofoten Low also results in a large-scale temperature oscillation between east Greenland and northern Scandinavia that has an amplitude of ~4°C. A similar large-scale temperature seesaw was identified by *van Loon and Rogers* [1978] using data from Oslo and Jacobshavn in west Greenland. This seesaw was attributed to variability associated with the NAO. Figure S4 in the supporting information confirms that this mode of variability does not have a large projection on the NAO.

A number of climate processes in the subpolar North Atlantic have been shown to be associated with variability in the Lofoten Low. These include sea ice conditions off the north coast of Iceland [*Kelly et al*., 1987], air-sea interaction over the Iceland Sea [*Moore et al*., 2012], and transport of sea ice through Fram Strait [*Jahnke-Bornemann and Bruemmer*, 2009; *Tsukernik et al*., 2010]. In particular, the latter process is consistent with the surface wind field associated with seesaw in sea ice identified in this paper. The existence of this new temperature oscillation and its association with the Lofoten Low is yet another indication of the important role that this circulation system plays in the climate of the region.

Acknowledgments

The AMSR-E sea concentration data set was provided by the University of Hamburg (http://icdc.zmaw.de/seaiceconcentration_asi_amsre.html), while the Bootstrap and NASA Team data sets were provided by the National Snow and Ice Data Center (http://nsidc.org). The ERA-1 reanalysis data set was provided by the European Centre for Medium-Range Weather Forecasts (http://www.ecmwf.int). The SST data set was provided by the NOAA/National Climate Data Center (http://www.ncdc.noaa.gov/sst/). G.W.K.M. was supported by the Natural Sciences and Engineering Research Council of Canada. F.S. and M.O. were supported by NSF OCE 1130008 and NASA NNX13AK88G. We thank the reviewers for their comments.

The Editor thanks Courtenay Strong and an anonymous reviewer for their assistance in evaluating this paper.

References

Andresen, C. S., et al. (2012), Rapid response of Helheim Glacier in Greenland to climate variability over the past century, *Nat. Geosci.*, *5*(1), 37–41.

Cavalieri, D. J., et al. (2013), *Sea Ice Concentrations From Nimbus-7 SMMR and DMSP SSM/I-SSMIS Passive Microwave Data*, Natl. Snow and Ice Data Cent., Boulder, Colo.

Chapman, W. L., and J. E. Walsh (1991), Long-range prediction of regional sea ice anomalies in the Arctic, *Weather Forecasting*, *6*(2), 271–288.

Christoffersen, P., et al. (2011), Warming of waters in an East Greenland fjord prior to glacier retreat: Mechanisms and connection to large-scale atmospheric conditions, *Cryosphere*, *5*(3), 701–714.

Comiso, J. C., and C. W. Sullivan (1986), Satellite microwave and in situ observations of the Weddell Sea ice cover and its marginal ice zone, *J. Geophys. Res.*, *91*(C8), 9663–9681, doi:10.1029/JC091iC08p09663.

Dee, D. P., et al. (2011), The ERA-Interim reanalysis: Configuration and performance of the data assimilation system, *Q. J. R. Meteorol. Soc.*, *137*(656), 553–597.

Deser, C., et al. (2000), Arctic sea ice variability in the context of recent atmospheric circulation trends, *J. Clim.*, *13*(3), 617–633.

Ghil, M., et al. (2002), Advanced spectral methods for climatic time series, *Rev. Geophys.*, *40*(1), 1003, doi:10.1029/2000RG000092.

Grebmeier, J. M., et al. (1995), Biological processes on Arctic continental shelves: Ice-ocean-biotic interactions, in *Arctic Oceanography: Marginal Ice Zones and Continental Shelves*, edited by W. O. Smith and J. M. Grebmeier, pp. 231–261, AGU, Washington, D. C., doi:10.1029/CE049p0231.

Hakkinen, S., and P. B. Rhines (2004), Decline of subpolar North Atlantic circulation during the 1990s, *Science*, *304*(5670), 555–559.

Holland, D. M., et al. (2008), Acceleration of Jakobshavn Isbrae triggered by warm subsurface ocean waters, *Nat. Geosci.*, *1*(10), 659–664.

Holton, J. R. (2004), An introduction to dynamic meteorology, in *International Geophysics Series Volume 88*, 535 pp., Elsevier Acad. Press, Burlington, Mass.

Howat, I. M., et al. (2011), Mass balance of Greenland's three largest outlet glaciers, 2000-2010, *Geophys. Res. Lett.*, *38*, L12501, doi:10.1029/2011GL047565.

Hurrell, J. W., and C. Deser (2009), North Atlantic climate variability: The role of the North Atlantic Oscillation, *J. Mar. Syst.*, *78*(1), 28–41.

Instanes, A. (2005), Infrastructure: Buildings, Support Systems, and Industrial Facilities, in *Arctic Climate Impact Assessment*, edited by J. Berner et al., Cambridge Univ. Press, Cambridge, U. K.

Jahnke-Bornemann, A., and B. Bruemmer (2009), The Iceland-Lofotes pressure difference: Different states of the North Atlantic low-pressure zone, *Tellus, Ser. A*, *61*(4), 466–475.

Kelly, P. M., et al. (1987), The interpretation of the Icelandic sea ice record, *J. Geophys. Res.*, *92*(C10), 10,835–10,843, doi:10.1029/JC092iC10p10835.

Kwok, R., et al. (2004), Fram Strait sea ice outflow, *J. Geophys. Res.*, *109*, C01009, doi:10.1029/2003JC001785.

Moore, G. W. K. (2012), Decadal variability and a recent amplification of the summer Beaufort Sea High, *Geophys. Res. Lett.*, *39*, L10807, doi:10.1029/2012GL051570.

Moore, G. W. K., et al. (2012), Spatial distribution of air-sea heat fluxes over the sub-polar North Atlantic Ocean, *Geophys. Res. Lett.*, *39*, L18806, doi:10.1029/2012GL053097.

Murray, T., et al. (2010), Ocean regulation hypothesis for glacier dynamics in southeast Greenland and implications for ice sheet mass changes, *J. Geophys. Res.*, *115*, F03026, doi:10.1029/2009JF001522.

Nuttall, M. (2005), Hunting, herding, fishing, and gathering: Indigenous peoples and renewable resource use in the Arctic, in *Arctic Climate Impact Assessment*, edited by J. Berner et al., Cambridge Univ. Press, Cambridge, U. K.

Oltmanns, M., et al. (2014), Strong Downslope Wind Events in Ammassalik, Southeast Greenland, *J. Clim.*, *27*(3), 977–993.

Parkinson, C. L., and D. J. Cavalieri (2008), Arctic sea ice variability and trends, 1979-2006, *J. Geophys. Res.*, *113*, C07004, doi:10.1029/2007JC004564.

Renfrew, I. A., and G. W. K. Moore (1999), An extreme cold-air outbreak over the Labrador Sea: Roll vortices and air-sea interaction, *Mon. Weather Rev.*, *127*(10), 2379–2394.

Reynolds, R. W., et al. (2007), Daily high-resolution-blended analyses for sea surface temperature, *J. Clim.*, *20*(22), 5473–5496.

Rudnick, D. L., and R. E. Davis (2003), Red noise and regime shifts, *Deep Sea Res., Part I*, *50*(6), 691–699.

Spreen, G., et al. (2008), Sea ice remote sensing using AMSR-E 89-GHz channels, *J. Geophys. Res.*, *113*, C02S03, doi:10.1029/2005JC003384.

Straneo, F., and P. Heimbach (2013), North Atlantic warming and the retreat of Greenland's outlet glaciers, *Nature*, *504*(7478), 36–43.

Straneo, F., et al. (2010), Rapid circulation of warm subtropical waters in a major glacial fjord in East Greenland, *Nat. Geosci.*, *3*(3), 182–186.
Straneo, F., et al. (2013), Challenges to understanding the dynamic response of Greenland's marine terminating glaciers to oceanic and atmospheric forcing, *Bull. Am. Meteorol. Soc.*, *94*(8), 1131–1144.
Strong, C. (2012), Atmospheric influence on Arctic marginal ice zone position and width in the Atlantic sector, February-April 1979-2010, *Clim. Dyn.*, *39*(12), 3091–3102.
Strong, C., and I. G. Rigor (2013), Arctic marginal ice zone trending wider in summer and narrower in winter, *Geophys. Res. Lett.*, *40*, 4864–4868, doi:10.1002/grl.50928.
Sutherland, D. A., and C. Cenedese (2009), Laboratory experiments on the interaction of a buoyant coastal current with a canyon: Application to the East Greenland Current, *J. Phys. Oceanogr.*, *39*(5), 1258–1271.
Sutherland, D. A., and R. S. Pickart (2008), The East Greenland Coastal Current: Structure, variability, and forcing, *Prog. Oceanogr.*, *78*(1), 58–77.
Sutherland, D. A., F. Straneo, and R. S. Pickart (2014), Characteristics and dynamics of two major Greenland glacial fjords, *J. Geophys. Res. Oceans*, *119*, 3767–3791, doi:10.1002/2013JC009786.
Tsukernik, M., et al. (2010), Atmospheric forcing of Fram Strait sea ice export: A closer look, *Clim. Dyn.*, *35*(7-8), 1349–1360.
van Loon, H., and J. C. Rogers (1978), Seesaw in winter temperatures between Greenland and Northern Europe. 1. General description, *Mon. Weather Rev.*, *106*(3), 296–310.
Walter, J. I., et al. (2012), Oceanic mechanical forcing of a marine-terminating Greenland glacier, *Ann. Glaciol.*, *53*(60), 181–192.